# Density of states of two-dimensional systems with long-range logarithmic interactions

Andrés M. Somoza,[1] Miguel Ortuño,[1] Tatyana I. Baturina,[2,3,4] and Valerii M. Vinokur[5]
[1]*Departamento de Física – CIOyN, Universidad de Murcia, Murcia 30.071, Spain*
[2]*University of Regensburg, Universitätsstraße 31, Regensburg 93053, Germany*
[3]*A. V. Rzhanov Institute of Semiconductor Physics SB RAS, 13 Lavrentjev Avenue, Novosibirsk 630090, Russia*
[4]*Department of Physics, Novosibirsk State University, 2 Pirogova Street, Novosibirsk 630090, Russia*
[5]*Materials Science Division, Argonne National Laboratory, 9700 S. Cass Avenue, Argonne, Illinois 60637, USA*
(Received 22 April 2015; published 3 August 2015)

We investigate a single-particle density of states (DOS) in strongly disordered two-dimensional high dielectric permittivity systems with logarithmic Coulomb interaction between particles. We derive self-consistent DOS at zero temperature and show that it is appreciably suppressed as compared to the DOS expected from the Efros-Shklovskii approach. We carry out zero- and finite-temperature Monte Carlo numerical studies of the DOS and find the perfect agreement between the numerical and analytical results at zero temperature, observing, in particular, a hardening of the Coulomb gap with the increasing electrostatic screening length. At finite temperatures, we reveal a striking scaling of the DOS as a function of energy normalized to the temperature of the system.

DOI: 10.1103/PhysRevB.92.064201 PACS number(s): 64.60.fd, 64.60.ah, 71.23.An, 72.20.Ee

## I. INTRODUCTION

Logarithmic interaction (LI) between superconducting vortices in bulk and two-dimensional (2D) superconductors [1] and Josephson junction arrays [2,3] governs their electromagnetic properties, resulting, most notably, in Berezinskii-Kosterlitz-Thouless (BKT) transition in films and Josephson junction arrays [4–8]. The vortex-vortex LI, which is referred to as 2D Coulomb interaction, holds on distances $r < \lambda$, where $\lambda = \lambda_{\perp}$ is the London penetration depth in bulk superconductors, and the Pearl screening length, $\lambda = \lambda_{P} = \lambda_{\perp}^2/a$, in thin films with $a$ being the film thickness. Since $\lambda_{\perp}$ is ordinarily of a macroscopic spatial scale (about microns), and $\lambda_{P}$ is even larger in thin films, the LI between vortices is a routine experimental situation, so that its fascinating consequences in vortex physics are explored in detail and understood fairly well. The effect of LI on the Coulomb gap and the variable range hopping conductivity was discussed in the context of vortex dynamics in Ref. [9].

With the 2D Coulomb interaction of charges the situation is different. The LI of charges in dielectric films endowed with the permeability higher than that of the surrounding was derived and discussed quite a while ago [10–12]. The possible effect of LI on hopping conductivity of electric charges was touched upon in Ref. [13]. Extensive numerical simulations of statistical properties of 2D arrays of single-electron islands with random background charges were carried out in Ref. [14], where it was demonstrated that LI noticeably affect the DOS and hopping conductivity, with both being system size dependent. However, the widespread orthodoxy is that in the realm of the experimental condensed matter the unscreened Coulomb interaction in dielectrics is always of the 3D nature, and so 2D charge Coulomb systems do not exist. At the same time, it was shown as early as in 1976 [15,16], see also Ref. [17], that near the 2D percolation metal-to-insulator transition the dielectric permeability diverges on approaching the transition from the insulating side. This effect was experimentally observed in many different systems, see, for example, Refs. [18–22]. This implies that in the critical vicinity of the metal-to-insulator and superconductor-to-insulator (SIT) transitions the long-range LI extends over macroscales, hence bringing in the charge BKT transitions at the respective insulating sides. As a fascinating denouement of a long-range LI effect, the critical vicinity of the SIT harbors two dual low-temperature BKT states, the superconducting one below the vortex BKT transition and, mirroring it, the superinsulating state below the charge BKT transition [3,23,24]. One of the most striking manifestations of the 2D Coulomb interaction is that the characteristic energy controlling the activation conductivity of the Cooper pair insulator scales as $E_a \propto \ln L$ [3,23,24], provided the size of the system, $L$, remains less than the electrostatic screening length $\Lambda$.

In parallel, a new class of 2D insulators with high dielectric permeability (often referred to as high-$\kappa$ sheets) has become one of the focuses of an extensive research, for they appeared of prime technological importance for the fabrication of nanoscale capacitor components in high-$\kappa$ devices, see Ref. [25], and references therein. One expects that since in high-$\kappa$ nanosheets $\Lambda \simeq \kappa a$ is of a macroscale size, the logarithmic charge interaction should essentially affect their electronic conductivity and DOS, which are key to the engineering high performance devices and the progress in their miniaturization. On the fundamental side, the interest is motivated by the challenge of understanding the behavior of a 2D Coulomb glass, a highly frustrated strongly correlated system whose properties are governed by the intertwined effects of disorder and the long-range LI [26]. An important step has been done in our previous publication [27] where hopping conductivity of a 2D Coulomb glass was investigated via a first-principles numerical study. We demonstrated that hopping transport is controlled by the characteristic energy that scales as $E_a \propto \ln \tilde{L}$ with $\tilde{L} = \min\{L, \Lambda\}$. One of the remaining mysteries of strongly disordered 2D insulators is their electronic DOS. A while ago, inspecting the effect of competition between the random potential localizing the electrons and the long-range electron-electron Coulomb interaction, Pollak [28] showed that the latter causes a deep depletion in the one-particle

 

DOS around the Fermi level. Efros and Shklovskii (ES) [29] offered an elegant single-particle treatment, having coined this depletion Coulomb gap. They found that for $V(r) \propto 1/r$, the DOS, $g(E)$, vanishes at the Fermi level as

$$g(E) \propto |E|^{d-1}, \tag{1}$$

where $d \geq 2$ is the dimensionality of the system. This $g(E)$ behavior is referred to as a soft gap. A self-consistent extension of the original calculation [30,31] allowed us to find the proportionality constants in different dimensions, $d/\pi$, [32] and yielded the same functional dependence of $g(E)$ in both $d = 2$ and 3 cases. The behavior of the DOS at finite $T$ was studied both analytically [33] and numerically [34,35] for a $1/r$ Coulomb interaction.

On the experimental side, there have been tantalizing reports revealing the intriguing behavior of the tunneling conductance and resistance in Be [36] and TiN [37] films in the close proximity to the SIT. The DOS was found to be temperature dependent evolving upon cooling from ES-like Coulomb gap to the hard gap at lowest temperatures in Be films. In TiN films in the critical vicinity of the SIT, the resistance exhibited an evolution from the ES law through activation to hyperactivation behavior [37] with decreasing temperature. This indicates that upon cooling down the ES-like gap transforms into a hard gap, ensuring activated conduction, and then the charge BKT occurs below which the resistance grows faster than exponentially with temperature. Furthermore, the hard gap was shown to broaden with the increase of the applied magnetic field. Although observed for quite some time, these fascinating behaviors of the Coulomb gap are still not understood. Here we step into the breach and relate them to the long-range LI of the unscreened charges in the 2D systems. We investigate the electronic DOS of 2D systems and, employing the self-consistent approach, find that the long-range 2D Coulomb interaction gives rise to the hard gaplike behavior in compliance with the experimental results by Refs. [36,37]. We carried out numerical studies of the DOS that yield the zero-temperature $g(E)$ perfectly agreeing with our analytical result. We also undertake a detailed Monte Carlo (MC) finite-temperature numerical study and find the temperature scaling of the DOS.

## II. THE MODEL

We consider a standard tight-binding Hamiltonian with long-range LI between carriers:

$$H = \sum_i Q_i e\phi_i + \sum_{i>j} \sum_j Q_i Q_j V(r_{i,j}). \tag{2}$$

Here, the charge $Q_i$ of the $i$th site is measured in units of the electron charge $e$, $\phi_i$ is the external potential at site $i$, and

$$V(r_{i,j}) = \begin{cases} E_0 \ln \frac{\Lambda}{r_{i,j}} & \text{if} \quad r_{i,j} < \Lambda \\ 0 & \text{if} \quad r_{i,j} \geqslant \Lambda \end{cases}, \tag{3}$$

where $E_0 = e^2/(2\pi\epsilon_0\kappa a)$ is the characteristic energy for the LI, $\kappa$ is the dielectric constant, $a$ is the thickness of the film, and $\Lambda = \min\{L/2, \kappa a\}$. We choose $\phi_i$ at random from the interval $[-B/2, B/2]$ and let the charge on each site $Q_i$ assume values $\pm 1/2$. This restriction lifts the on-site charging effects, but does not affect the generality of the results. The Hamiltonian exhibits the particle-hole symmetry and so the chemical potential is $\mu = 0$.

The electrostatic site energies are given by

$$\epsilon_i = e\phi_i + \sum_{j \neq i} Q_j V(r_{i,j}), \tag{4}$$

and DOS is defined as $g(E) = \langle \delta(\epsilon_i - E) \rangle_i$, where averaging is taken over all sites $i$. The excitation energy corresponding to a single electron $i \to j$ hop is

$$\Delta_{i,j} = \epsilon_j - \epsilon_i - V(r_{i,j}). \tag{5}$$

In the ground state, the stability criterion $\Delta_{i,j} \geq 0$ results in a gap in the DOS. Extending the standard arguments of Efros and Shklovskii for the Coulomb gap [29] onto the LI in 2D, one gets the exponential gap in the DOS as

$$g(E) = \frac{4}{\pi \Lambda^2 E_0} \exp\left(\frac{2|E|}{E_0}\right), \tag{6}$$

where the prefactor was obtained, in the context of the vortex DOS, by Taüber and Nelson [38] (hereafter we will be referring to this formula as to TN). Note that the screening length enters Eq. (6) through the prefactor only.

## III. SELF-CONSISTENT CALCULATION

At variance with the Coulomb gap generated by the $1/r$ interaction, the self-consistency in the case of the LI in 2D results in a new functional form of the DOS energy dependence. The self-consistent DOS is defined by the integral equation [30,31]

$$g(E) = g_0 \exp\left[-2\pi \int_{-\infty}^{0} dE' g(E') \int_0^{V^{-1}(E-E')} r\, dr\right], \tag{7}$$

where $g_0 = 1/B$ is the DOS in the system without interactions and measures the degree of disorder. The exponential factor in Eq. (7) is the probability that in the neighborhood of a given site there are no other sites breaking the particle-hole stability criterion. The upper integration limit refers to the inverse function of the interaction potential and is equal to $V^{-1}(E) = \Lambda \exp\{-E/E_0\}$. Integrating over $r$ the exponent in Eq. (7) gives rise to

$$g(E) = g_0 \exp\left[-\pi \Lambda^2 \int_{-\infty}^{0} dE' g(E') e^{-2(E-E')/E_0}\right]. \tag{8}$$

The factor $\exp(-2E/E_0)$ can be taken out of the integral over $E'$, and reduces to a constant, $b$, independent of $E$ and given by the self-consistent equation

$$b = g_0 \frac{E_0}{2\pi \Lambda^2 b}\left(1 - e^{-\pi \Lambda^2 b}\right). \tag{9}$$

Neglecting the small second term in the brackets, one arrives at the self-consistent expression for the DOS:

$$g(E) = g_0 \exp\left(-\Lambda \sqrt{\frac{\pi g_0 E_0}{2}} e^{-2|E|/E_0}\right). \tag{10}$$

Equation (10) is the central result of our paper.

One immediately discerns that the gap is no longer universal since it depends strongly on the unperturbed DOS, $g_0$, and on

the screening length, $\Lambda$. In the limit $E \ll E_0$, one can expand $\exp(-2|E|/E_0)$ in Eq. (10) to recover the exponential gap

$$g(E) \approx g_0 \exp\left(-\Lambda\sqrt{\frac{\pi g_0 E_0}{2}}\right) \exp\left(\Lambda|E|\sqrt{\frac{2\pi g_0}{E_0}}\right), \quad (11)$$

which differs noticeably from the non-self-consistent result of Eq. (6). In Eq. (11), both, the pre-exponential factor and the exponent, depend on $g_0$ and $\Lambda$.

## IV. NUMERICAL RESULTS AT ZERO TEMPERATURE

To compute the DOS, we run a numerical algorithm that relaxes the system into a state stable against all single-particle transitions (but metastable with respect to simultaneous many-particle transitions) [39]. We take an arbitrary random configuration of occupied and empty sites and change the site occupations until all occupied sites acquire negative energy and all empty sites acquire positive energy. Then we exercise the particle-hole transitions that decrease the energy of the system (and return to the first part of the algorithm that relaxes by changing individual sites occupation) until the system becomes stable against all particle-hole transitions. Then we make a histogram of the site energies and average the result over at least $10^4$ realizations of disorder.

In Figs. 1(a) and 1(b), we show the $g(E)$ in logarithmic and linear scales for four different system sizes and disorder amplitude $B = 10$ and $\Lambda = 10$. Hereafter, $E$ and all the quantities of dimensionality of the energy are measured in the units of $E_0$. The data indicate a practical absence of dependence of $g(E)$ on the system size, provided $L \gg \Lambda$. The solid line depicts the DOS calculated from our self-consistent Eq. (10) without any adjustable parameters and fits pretty well the numerical results. The minuscule discrepancy between the numerical results and analytical expression stemming from neglecting the exponential correction in Eq. (9) is mended by the small change of the parameters $g_0$ and $\Lambda$. The TN dotted line stands for the DOS obtained in TN approximation, see Eq. (6). The TNS line is calculated from Eq. (6), where instead of the numerical factor 2 in the exponent, we took the factor 4 according to Ref. [40]. One sees that these curves, obtained in the framework of the ES theory, deviate noticeably from the simulation data. Figure 1(c) shows the DOS for different screening lengths, while keeping the ratio $L/\Lambda$ constant. Remarkably, the increase in $\Lambda$ results in essential broadening of the $g(E)$ curves. This resembles the experimental results evidencing the broadening of the hard gap upon increasing the applied magnetic field in Be films [36]. Note that this trend is exactly what is expected to occur in disordered superconducting films as they fall into the critical vicinity of the SIT where their dielectric constant drastically increases. For high-dielectric sheets, beyond the screening length, there is an unscreened Coulomb $1/r$ interaction. Strictly speaking, this unscreened tail contributes to the low-energy part of the DOS and close enough to Fermi level the DOS acquires a linear shape. However, at realistic parameters the energy interval of linear behavior of the DOS is narrow and barely detectable in the experiment.

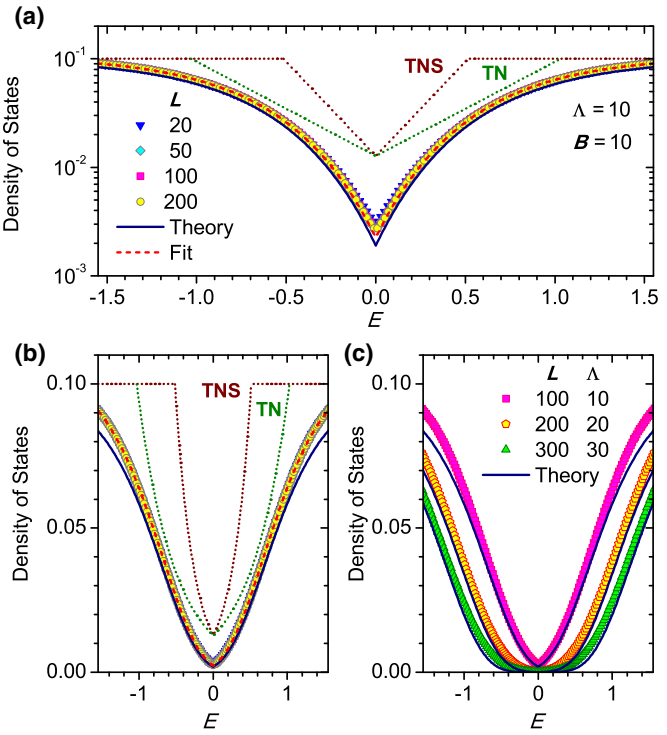


FIG. 1. (Color online) Density of states vs energy at maximal strength of disorder $B = 10$. (a) and (b) present the same numerical data for different sample sizes and $\Lambda = 10$ in the logarithmic and linear scales, respectively. The legend given in the panel (a) is common for both (a) and (b). The numerical data are shown by symbols. The dotted line marked as TN is the DOS according to Eq. (6) and the dotted line marked as TNS is the line that accounts for the exponent found in Ref. [40] [keeping the prefactor of Eq. (6)]. The solid line is our self-consistent result of Eq. (10), with $g_0 \equiv 1/B = 0.1$ and $\Lambda = 10$. The dashed line is the fit by Eq. (10), with $g_0 = 0.108$ and $\Lambda = 9.4$. (c) The DOS, $g(E)$, for three different values of $\Lambda$, at fixed ratio $L/\Lambda = 10$. Numerical data are shown by symbols, the solid lines present the fit by Eq. (10) with the respective $\Lambda$-s and $g_0 = 0.1$.

## V. FINITE-TEMPERATURE RESULTS

To study the temperature evolution of the DOS, we carry out extensive Monte Carlo simulations. Starting our procedure from an arbitrary random configuration of charges, we equilibrate it at some relatively high temperature $T_1$ utilizing the standard MC procedure. Then we set the lower temperature $T_2 < T_1$ and exercise the equilibration procedure with the larger number of the MC steps. Repeating this operation successively we reach the temperature $T = 0.05$ at which the equilibration of the system becomes extremely slow, so that it would have taken weeks to make one more step down in temperature. Figure 2(a) and 2(b) present the color plots of the results of the simulations in the temperature range $T < E_0$. One observes the drastic dependence of the DOS on temperature, with the filling of the gap up to energies $\sim T$. This is to be expected, since temperature smooths down the small barriers between the energy minima. Hence one can expect that at $E, T \ll E_0$ the temperature sets the scale of the energy and therefore $g(E = 0, T) = g(cT, 0)$, with $c$ being

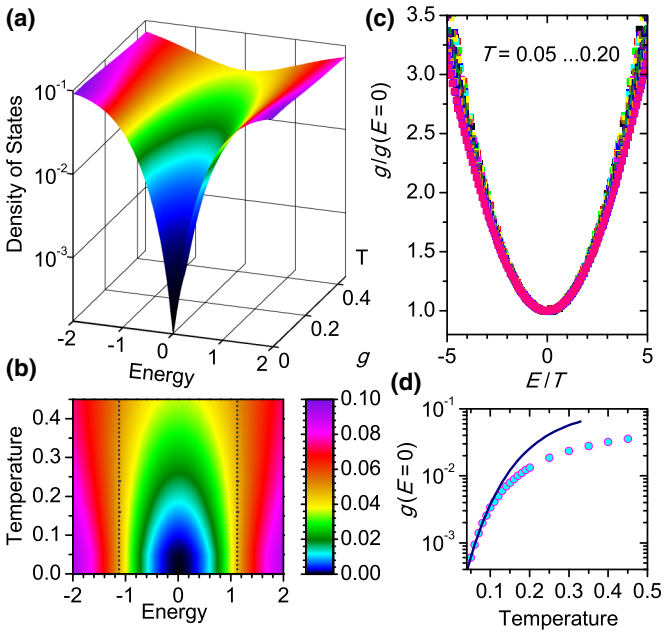


FIG. 2. (Color online) Temperature dependence of the DOS calculated at $L = 50$, $\Lambda = 20$, and $B = 10$. Three-dimensional (a) and two-dimensional (b) color plots of numerical data for $g(E,T)$. (c) Numerical data for the DOS normalized by the $g(E = 0)$ as a function of the energy-to-temperature ratio, $E/T$. Plot comprises 16 curves calculated in the temperature interval from $T = 0.05$ to $T = 0.20$ with the temperature step of 0.01. (d) $g(E = 0)$ vs temperature (symbols). The solid line presents the fit by Eq. (10), where $E = 4.4T$, $\Lambda = 20$, and $g_0 = 0.1$.

the constant. Figure 2(b) clearly shows the elliptical shape of the iso-$g$ lines centered at $E = 0$, $T = 0$. One further sees that the ratio between the large and small semiaxis of ellipses is about 4. The states with large energies $E \gtrsim E_0$ are not smoothed down by temperature, the transition between these domains of different temperature behaviors is marked by the dashed lines. Close inspection of the data reveals the striking scaling behavior of the DOS. Plotting $g(E,T)/g(0,T)$ as a function of $E/T$ demonstrates an excellent collapse of all the curves onto a single scaling dependence, which for this case is roughly parabolic, see Fig. 2(c). The plot $g(E = 0,T)$ shown in Fig. 2(d) by symbols is well fitted by Eq. (10) at $T < 0.1$, where $E$ is substituted by $cT$, with $c = 4.4$. The exact form of scaling function for $g(E,T)$ that applies over all energy and temperature range is at present not available and will be a subject of a forthcoming study.

To summarize, 2D systems endowed with the long-range LI exhibit a vast richness of fascinating properties. The zero temperature self-consistent DOS displays a hard gaplike behavior in an excellent agreement with our numerical results and differs significantly from the orthodox ES $g(E)$. Our finite-temperature numerical study has demonstrated a striking scaling of $g(E,T)$ as a function of $E/T$ in a finite energy interval from $-E_0/T$ to $E_0/T$ [35,41]. This scaling possibly reflects a thermal reconstruction of the energy spectrum of the low-temperature phase of the Coulomb glass, where temperature plays the role of the characteristic energy scale. The next immediate task is including the self-consistent consideration into the scheme of the description of the variable range hopping transport. We expect that LI is relevant over a wide temperature range [42], where a hopping distance controlling the variable range hopping logarithmically depends on the temperature [26]. The long-range character of the LI is likely to enhance the importance of the simultaneous many-electron jumps [43], which may be relevant for the understanding of glassy relaxation in electronic systems [44,45]. The important subclass of 2D systems with high dielectric permittivity are superconducting films in the critical vicinity of the SIT. The logarithmically size-dependent activation energy has been indeed found experimentally in InO and TiN films [3,23]. Finding the finite-temperature self-consistent $g(E,T)$ in 2D systems with the long-range LI and exploring its role in the mechanism of the superconductor- and metal-insulator transitions poses the next upcoming challenge.

## ACKNOWLEDGMENTS

The work was supported by the MINECO (Spain) and FEDER (EU) Grant No. FIS2012-38206; by the Ministry of Education and Science of the Russian Federation and by the Alexander von Humboldt Foundation (T.B.); and by the US Department of Energy, Office of Science, Materials Sciences and Engineering Division (V.V. and partly M.O. and T.B. via the Materials Theory Institute). M.O. thanks Kavli Institute of Theoretical Physics (KITP), University of California, Santa Barbara for hospitality.

[1] A. A. Abrikosov, *Fundamentals of the Theory of Metals* (North-Holland, Amsterdam, 1988).
[2] R. Fazio and H. van der Zant, Phys. Rep. **355**, 235 (2001).
[3] T. I. Baturina and V. M. Vinokur, Ann. Phys. **331**, 236 (2013).
[4] V. L. Berezinskii, Zh. Eksp. Teor. Fiz. **59**, 907 (1970) [Sov. Phys. JETP **32**, 493 (1971)].
[5] V. L. Berezinskii, Zh. Eksp. Teor. Fiz. **61**, 1144 (1971) [Sov. Phys. JETP **34**, 610 (1972)].
[6] J. M. Kosterlitz and D. J. Thouless, J. Phys. C **6**, 1181 (1973).
[7] P. Minnhagen, Rev. Mod. Phys. **59**, 1001 (1987).
[8] For a recent review, see *40 Years of Berezinskii-Kosterlitz-Thouless Theory*, edited by Jorge V. José (World Scientific, Singapore, 2013).
[9] D. R. Nelson and V. M. Vinokur, Phys. Rev. B **48**, 13060 (1993).
[10] N. S. Rytova, Vestnik MSU (in Russian) **3**, 30 (1967).
[11] A. V. Chaplik and M. V. Entin, Zh. Eksp. Teor. Fiz. **61**, 2496 (1971) [Sov. Phys. JETP **34**, 1335 (1972)].
[12] L. V. Keldysh, JETP Lett. **29**, 658 (1979) [Pisma Zh. Eksp. Teor. Fiz. **29**, 716 (1979)].
[13] A. I. Larkin and D. E. Khmelnitskii, Zh. Eksp. Teor. Fiz. **83**, 1140 (1982) [Sov. Phys. JETP **56**, 647 (1982)].
[14] D. M. Kaplan, V. A. Sverdlov, and K. K. Likharev, Phys. Rev. B **68**, 045321 (2003).
[15] V. E. Dubrov, M. E. Levinstein, and M. S. Shur, Zh. Eksp. Teor. Fiz. **70**, 2014 (1976) [Sov. Phys. JETP **43**, 1050 (1976)].

[16] A. L. Efros and B. I. Shklovskii, Phys. Stat. Sol. **76**, 475 (1976).
[17] Y. Imry, Y. Gefen, and D. J. Bergman, Phys. Rev. B **26**, 3436 (1982).
[18] T. G. Castner, N. K. Lee, G. S. Cieloszyk, and G. L. Salinger, Phys. Rev. Lett. **34**, 1627 (1975).
[19] D. M. Grannan, J. C. Garland, and D. B. Tanner, Phys. Rev. Lett. **46**, 375 (1981).
[20] H. F. Hess, K. DeConde, T. F. Rosenbaum, and G. A. Thomas, Phys. Rev. B **25**, 5578 (1982).
[21] A. I. Yakimov and A. V. Dvurechenskii, JETP Lett. **65**, 354 (1997).
[22] M. Watanabe, K. M. Itoh, Y. Ootuka, and E. E. Haller, Phys. Rev. B **62**, R2255 (2000).
[23] M. V. Fistul, V. M. Vinokur, and T. I. Baturina, Phys. Rev. Lett. **100**, 086805 (2008).
[24] V. M. Vinokur, T. I. Baturina, M. V. Fistul, A. Yu. Mironov, M. R. Baklanov, and C. Strunk, Nature **452**, 613 (2008).
[25] M. Osada and T. Sasaki, Adv. Mater. **24**, 210 (2012).
[26] M. Pollak, M. Ortuño, and A. Frydman, *The Electron Glass* (Cambridge University Press, Cambridge, 2013).
[27] M. Ortuño, A. M. Somoza, V. M. Vinokur, and T. I. Baturina, Sci. Rep. **5**, 9667 (2015).
[28] M. Pollak, Discuss. Faraday Soc. **50**, 13 (1970).
[29] A. L. Efros and B. I. Shklovskii, J. Phys. C **8**, L49 (1975).
[30] A. L. Efros, J. Phys. C **9**, 2021 (1976).
[31] M. E. Raikh and A. L. Efros, JETP Lett. **45**, 280 (1987) [Pisma Zh. Eksp. Teor. Fiz. **45**, 225 (1987)].
[32] S. D. Baranovskii, B. I. Shklovskii, and A. L. Efros, Zh. Eksp. Teor. Fiz. **78**, 395 (1980) [Sov. Phys. JETP **51**, 199 (1980)].
[33] A. A. Mogilyansky and M. E. Raikh, Zh. Eksp. Teor. Fiz. **95**, 1870 (1989) [Sov. Phys. JETP **68**, 1081 (1989)].
[34] F. G. Pikus and A. L. Efros, Phys. Rev. Lett. **73**, 3014 (1994).
[35] M. Goethe and M. Palassini, Phys. Rev. Lett. **103**, 045702 (2009).
[36] E. Bielejec, J. Ruan, and W. Wu, Phys. Rev. Lett. **87**, 036801 (2001).
[37] T. I. Baturina, A. Yu. Mironov, V. M. Vinokur, M. R. Baklanov, and C. Strunk, JETP Lett. **88**, 752 (2008).
[38] U. C. Täuber and D. R. Nelson, Phys. Rev. B **52**, 16106 (1995).
[39] A. Pérez-Garrido, M. Ortuño, A. Díaz-Sánchez, and E. Cuevas, Phys. Rev. B **59**, 5328 (1999).
[40] B. I. Shklovskii, arXiv:0803.3331.
[41] Note that earlier numerical studies of the 3D case [35] also revealed scaling of $g(E,T)$. However, the scaling of Ref. [35] appeared to work only at intermediate energies.
[42] J. Delahaye, T. Grenet, and F. Gay, Eur. Phys. J. B **65**, 5 (2008); T. Grenet, *ibid.* **32**, 275 (2003).
[43] A. M. Somoza, M. Ortuño, and M. Pollak, Phys. Rev. B **73**, 045123 (2006); J. Bergli, A. M. Somoza, and M. Ortuño, *ibid.* **84**, 174201 (2011).
[44] A. L. Burin and A. K. Kurnosov, J. Low Temp. Phys. **167**, 318 (2012).
[45] A. M. Somoza, M. Ortuño, M. Caravaca, and M. Pollak, Phys. Rev. Lett. **101**, 056601 (2008).